TROPOSPHERIC MOISTURE CONTENT OVER EUROPE
- A CLIMATOLOGICAL PERSPECTIVE -

Agnieszka WYPYCH

Jagiellonian University, Department of Climatology (Institute of Geography and Spatial Management)
Institute of Meteorology and Water Management – National Research Institute, Department of Meteorology, Climatology and Atmosphere Protection

Kraków – Warszawa, 22 January 2021

- A CLIMATOLOGICAL PERSPECTIVE -

- WHY THE WATER VAPOUR -

Its importance in the atmospheric processes

- ✓hydrological cycle
- ✓circulation systems
- ✓radiation and energy balance
- ✓climate change

Numerous number of moisture variables

Climatologically less recognized

- STATE-OF-THE-ART -

Measuring / acquiring methods : Wong i in. 2015; Forth et al. 2015; Fedele et al. 2015; …

Physical properties of tropospheric water vapour : Rosen & Imolayo 1981; Salstein et al. 1983; Sugiyama et al. 2005; Giaotti & Stel 2006; Harrison & Aplin 2007; Linné et al. 2007; Trenberth et al. 2011; Write et al. 2011; Pokam et al. 2012; Fueglistaler et al. 2013; Backes et al. 2015; Ryu et al. 2015; Vogelmann et al. 2015; Virts & Houze 2015; Lavers & Villarini 2015; …

Vertical structure of atmospheric moisture content : Pierrehumbert et al. 2007; Holloway & Neelin 2009; Kim et al. 2009; Paltridge et al. 2009; Devasthale et al. 2011; Tomasi et al. 2011; Valea et al. 2012; Ortiz de Galisteo et al. 2014; Sivira et al. 2015; Blumberg et al. 2015; Louf et al. 2015; Bordi et al. 2015; …

Spatial differentiation of tropospheric water vapour : Tuller 1968; Trenberth & Guillemot 1995; Bohoye et al. 2003; Gettelman et al. 2006; Jin et al. 2008; Zveryaev II et al. 2008; Jin & Luo 2009; Morland i in 2009; Rinke et al. 2009; van der Ent et al. 2010; Willet et al. 2010; Simmons et al. 2010; Valea et al. 2012; Raddatz et al. 2013; Wong et al. 2015; Forth et al. 2015; …

Temporal variability of tropospheric water vapour : Bates & Jackson 2001; Bates et al. 2001; Trenberth et al. 2005; Schiano et al. 2005; Wagner et al. 2006; Kassomenos & McGregor 2006; Vincent 2007; Ryoo et al. 2008; Willet et al. 2008; Zveryaev II et al. 2008; Mieruch et al. 2008; Jakobson et al. 2009; Rinke et al. 2009; Paltridge et al. 2009; Zhang et al. 2010; Sherwood et al. 2010; Jung et al. 2010; Simmons et al. 2010; Mattar et al. 2011; Ortiz de Galisteo et al. 2011, 2014; Willet et al. 2013, 2014; Louf et al. 2015; …

Moisture transport : Hutchings 1961; Salstein i in. 1983; Jedlovec i in. 2000; Turato i in. 2004; Linné i in. 2007; Bisselink & Dolman 2008; Tietäväninen & Vihma 2008; Yang i in 2008; Chow i in. 2008; Arraut & Salyamurty 2009; Sodemann i in. 2009; Jakobson & Vihma 2010; Li i in. 2011, 2012; Wang i in. 2014; Conto i in. 2015; Lavers & Villarini 2015; Ryu i in. 2015; Huang & Cui 2015; ...

- AIM OF THE STUDY -

Assessment of the amount of water vapor in troposphere over Europe and North-Eastern part of the Atlantic Ocean – its temporal and spatial differentiation → **tropospheric water vapour climatology**

- ✓ Moisture content regionalisation including spatial patterns and vertical profiles
- ✓ Atmospheric circulation importance in formation and/or modification of moisture conditions

- DATA -

ERA-Interim REANALYSES
European Centre for Medium-Range Weather Forecasts, ECMWF

01.01.1981 – 31.12.2015 daily data

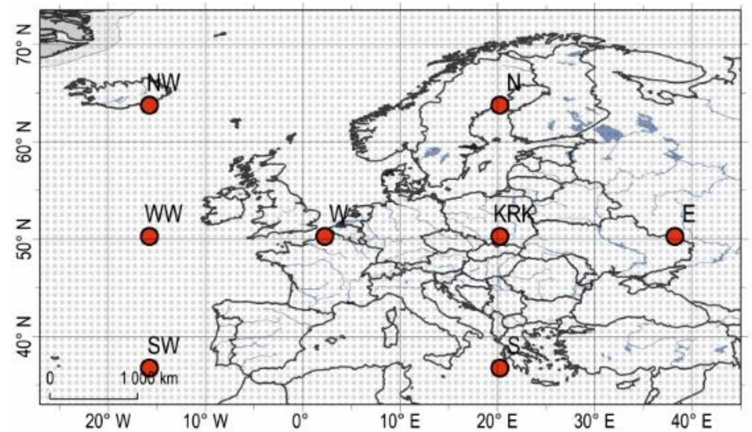

Europe & NE Atlantic
27°W – 45°E & 33°N – 73,5°N
Greenland excluded

spatial resolution: 0.75° x 0.75°

Surface: total column water vapour (TCWV)
relative humidity (RH)
sea level pressure (SLP)
wind (Uw, Vw)

pressure levels:

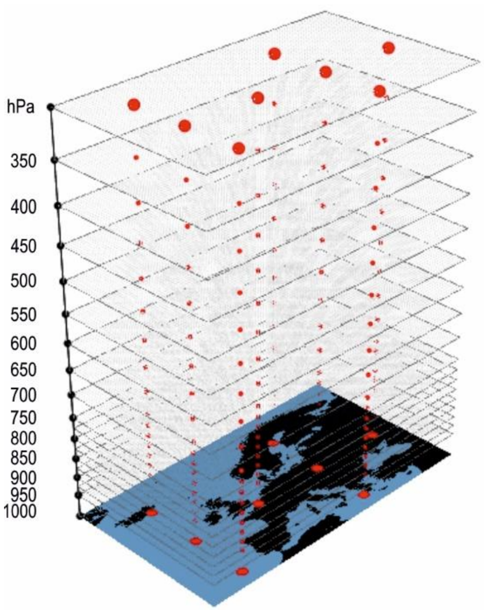

300 hPa
350 hPa
400 hPa
450 hPa
500 hPa
550 hPa
600 hPa
650 hPa
700 hPa
725 hPa
750 hPa
775 hPa
800 hPa
825 hPa
850 hPa
875 hPa
900 hPa
925 hPa
950 hPa
~~975 hPa~~
~~1000 hPa~~

specific humidity (SHUM or q)
relative humidity (RH)
geopotential height
wind (Uw, Vw)

- WORKFLOW / METHODS / RESULTS -

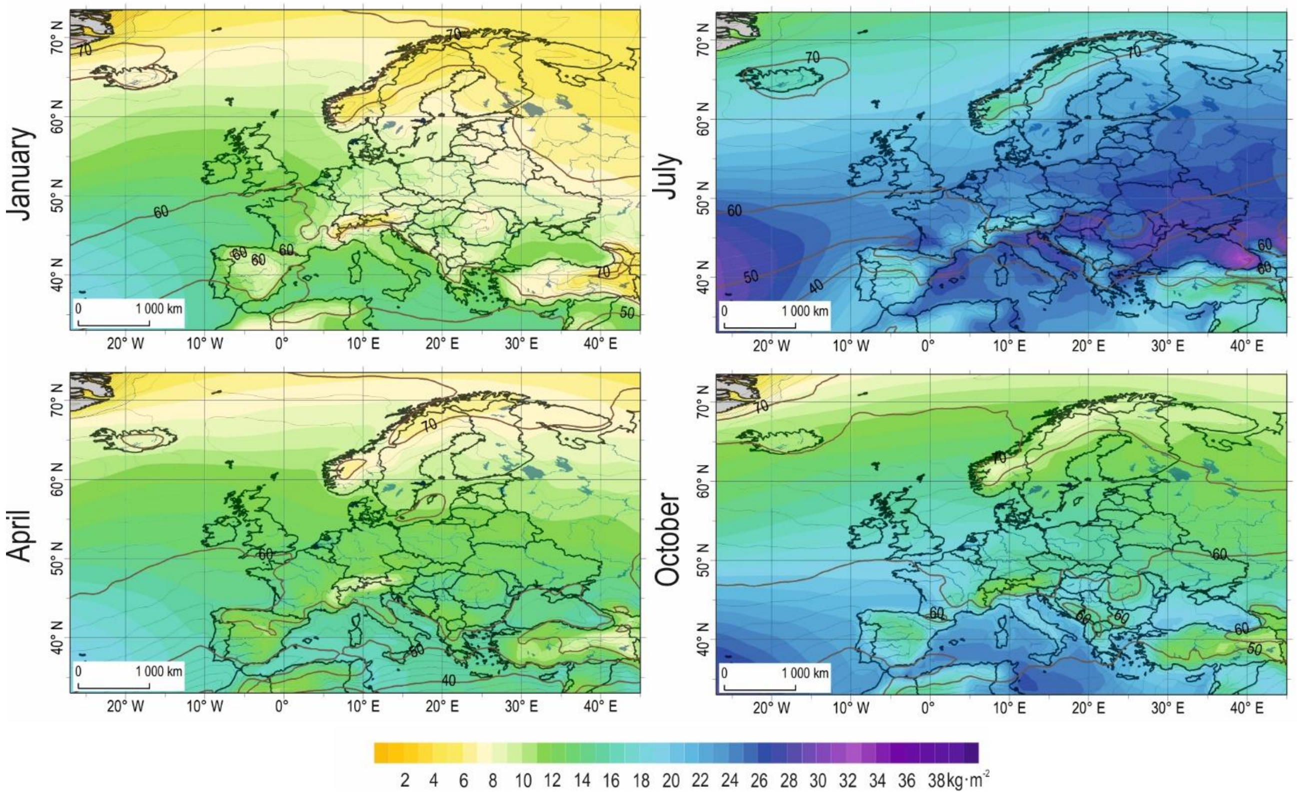

Climatology of monthly water vapor content in the atmosphere (TCWV) (kg·m^{-2}, coloured) and relative humidity (RH) (%, solid lines) (1981–2015)

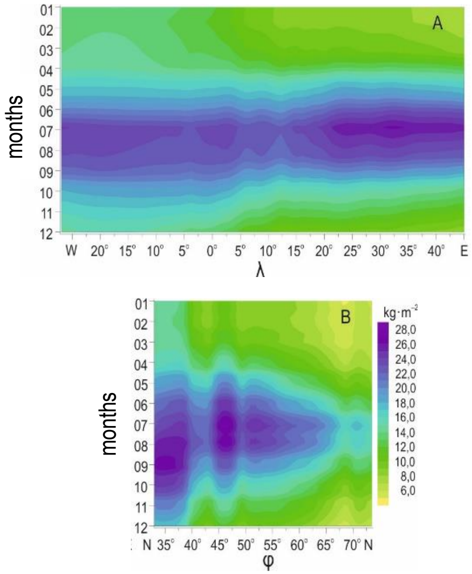

Annual distribution of tropospheric moisture content (TCWV, kg·m^{-2}):

A) cross-section along 50.25°N
B) cross-section along 20.25°E

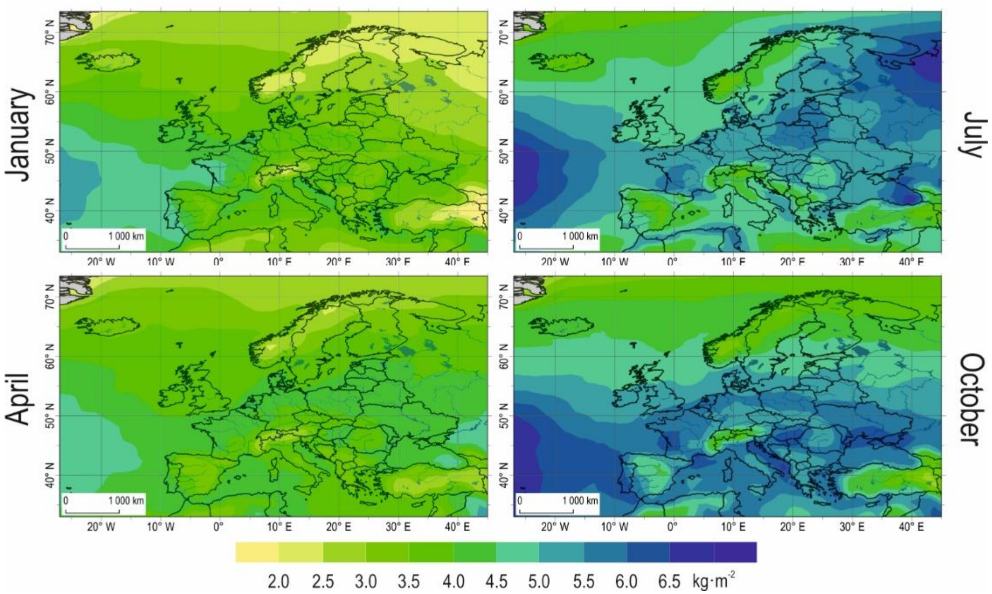

Standard deviations (SD) of monthly TCWV values (kg·m^{-2}) (1981-2015)

Spatial patterns

principal component analysis, PCA

empirical orthogonal function, EOF

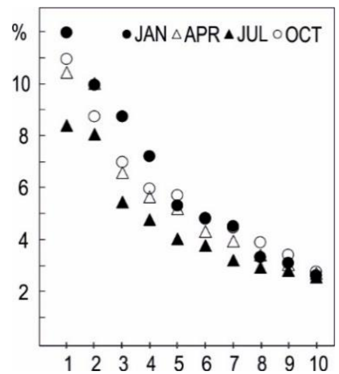

Amount of variance (%) explained by EOF modes 1–10 for selected months (1981–2015)

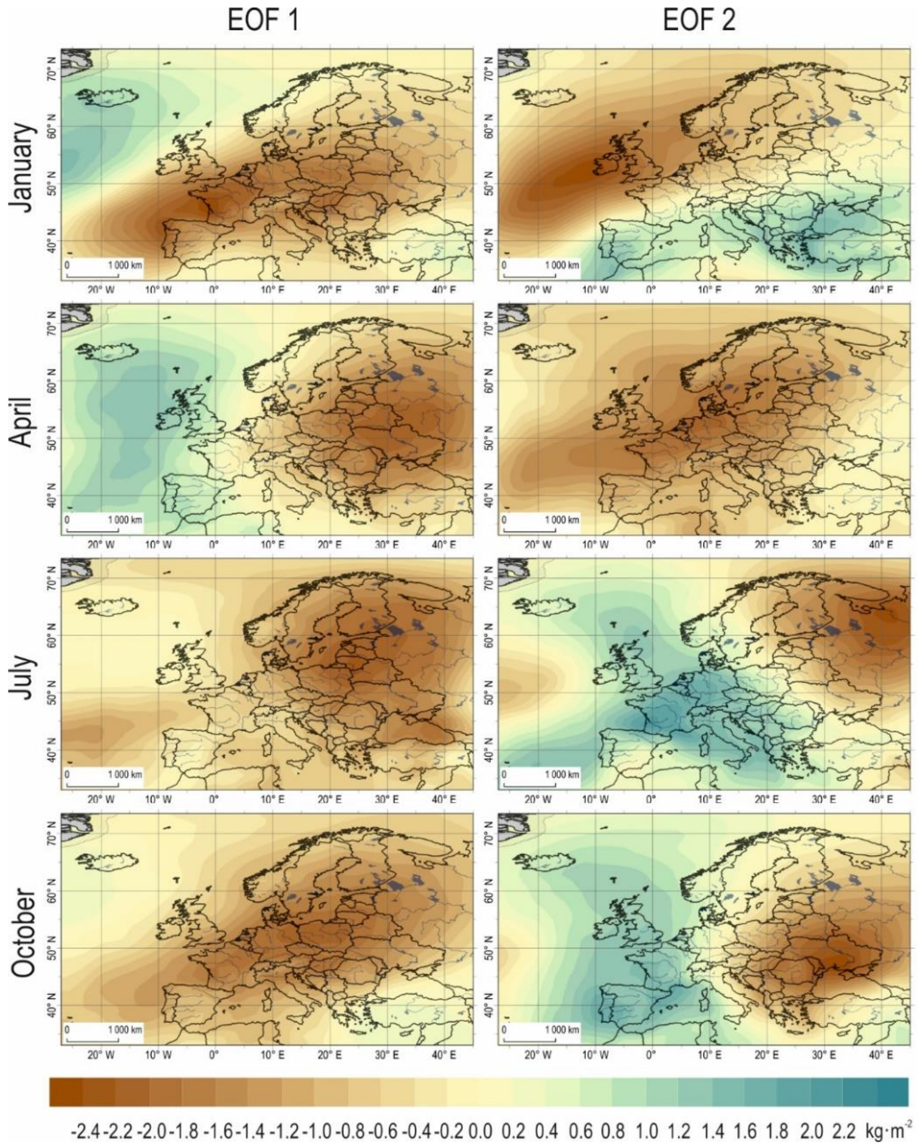

Spatial patterns of TCWV anomalies (kg·m^{-2}) in selected months for two leading EOF modes (1981–2015)

Vertical patterns

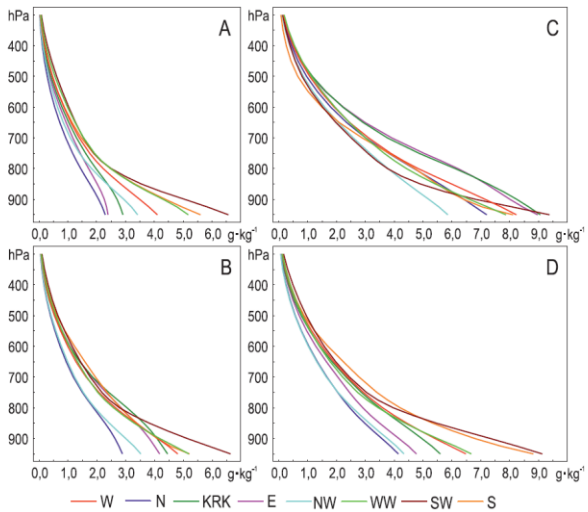

SHUM vertical profiles in particular grid points in selected months:
A) JAN, B) APR,
C) JUL, D) OCT

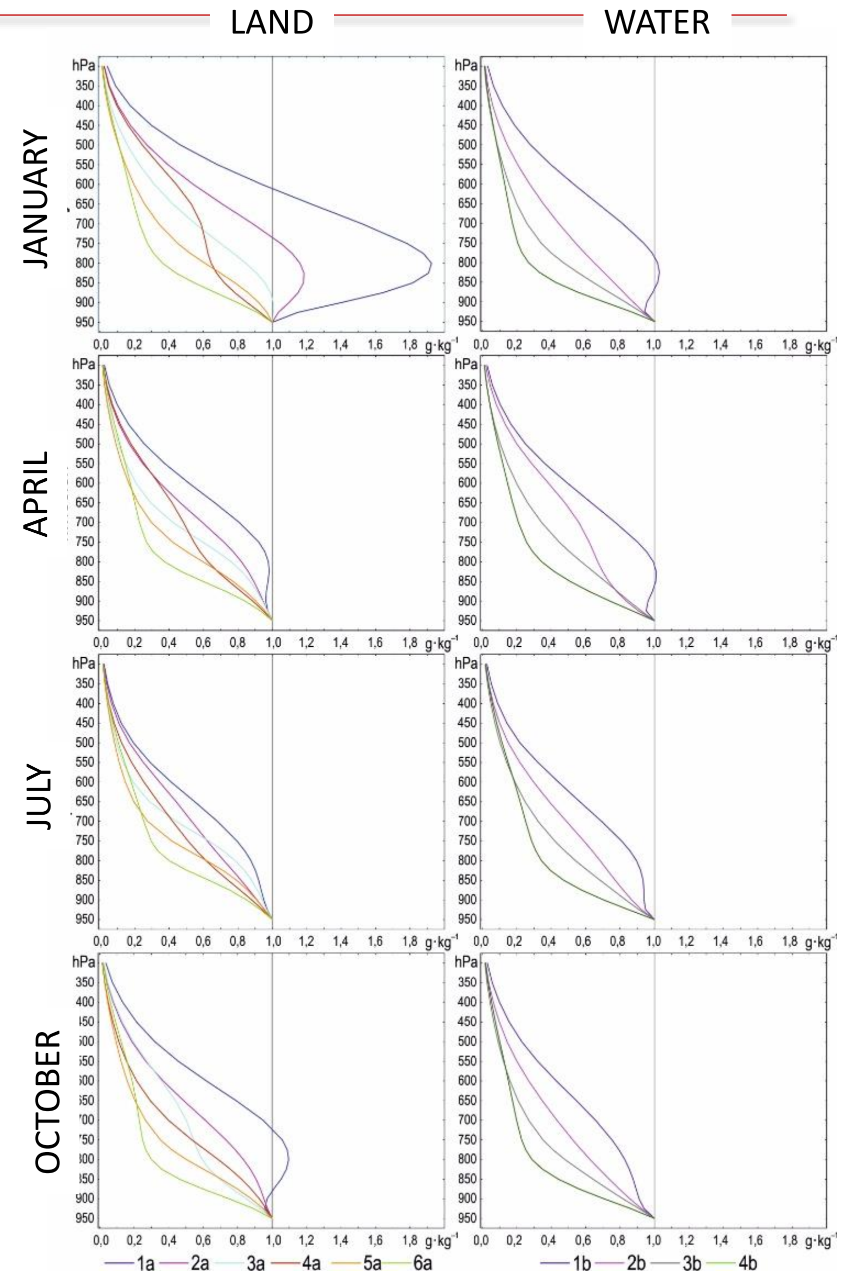

exploratory data analysis, EDA

SHUM gradient → land / water

- PCA
- V-fold cross-validation
- Pseudo-F statistics

k-means method

RMS difference ratio, RDR

$$RDR = \frac{\sum_{l=1}^{K}\sum_{k=1}^{K} N_k N_l}{\sum_{k=1}^{K} N_k (N_k - 1)} \cdot \frac{\sum_{k=1}^{K} \sum_{j=1}^{N_k} \sum_{i=1}^{N_k} S(x_{ik}, x_{jk})}{\sum_{l=1}^{K} \sum_{k=1}^{K} \sum_{j=1}^{N_l} \sum_{i=1}^{N_k} S(x_{ik}, x_{jl})}, l \neq k$$

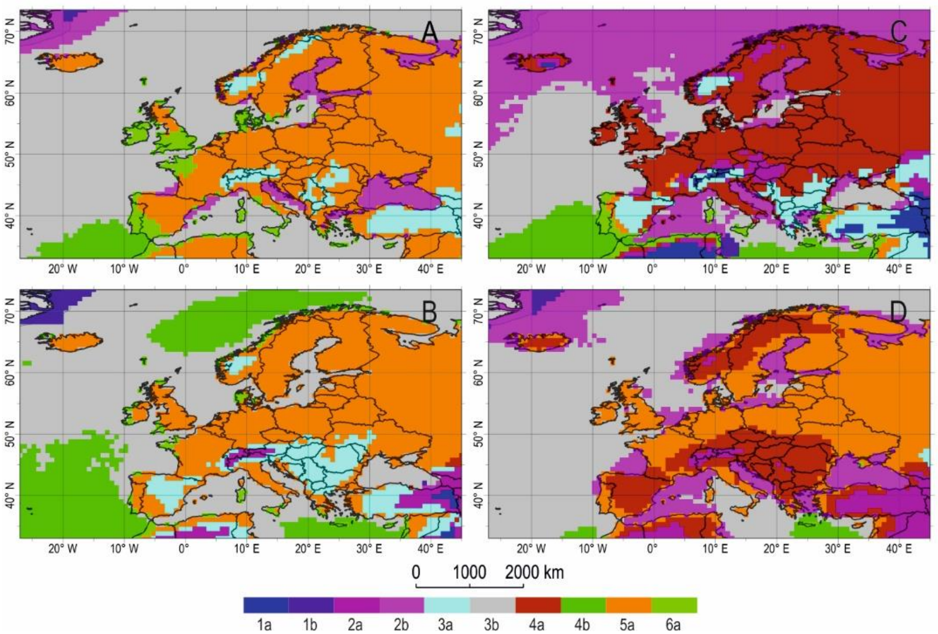

The most frequent types in selected months: A) JAN, B) APR, C) JUL, D) OCT

RDR values for distinguished types in selected months

types		months			
		01	04	07	10
land	1a	0,617	0,356	0,594	0,413
	2a	0,487	0,333	0,347	0,397
	3a	0,371	0,301	0,406	0,419
	4a	0,418	0,388	0,311	0,314
	5a	0,296	0,331	0,364	0,296
	6a	0,359	0,477	0,616	0,427
water	1b	1,074	0,915	0,667	0,724
	2b	0,478	0,439	0,331	0,375
	3b	0,342	0,427	0,322	0,330
	4b	0,450	0,422	0,521	0,472

Moisture inversions

$$QIS = \frac{q(p_{min}) - q(p_{max})}{|p_{min} - p_{max}|}$$

QIS – inversion strength [$kg \cdot kg^{-1} \cdot m^{-1}$]

q – specific humidity [$kg \cdot kg^{-1}$]

p_{min} – the height of the inversion top [m]

p_{max} – the height of the inversion base [m]

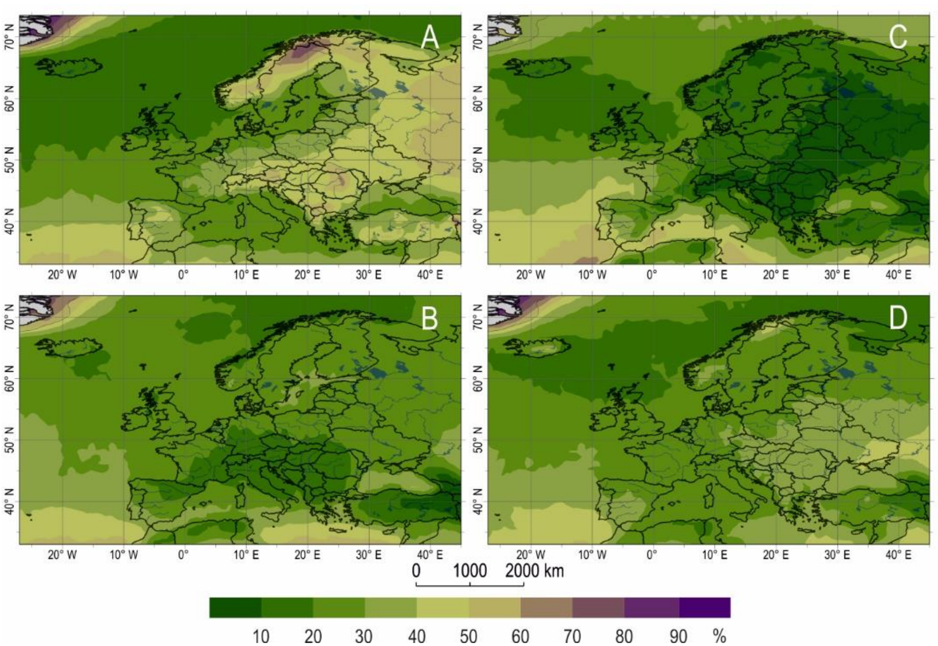

Frequency [%] of humidity inversions occurrence
in selected months: A) JAN, B) APR, C) JUL, D) OCT

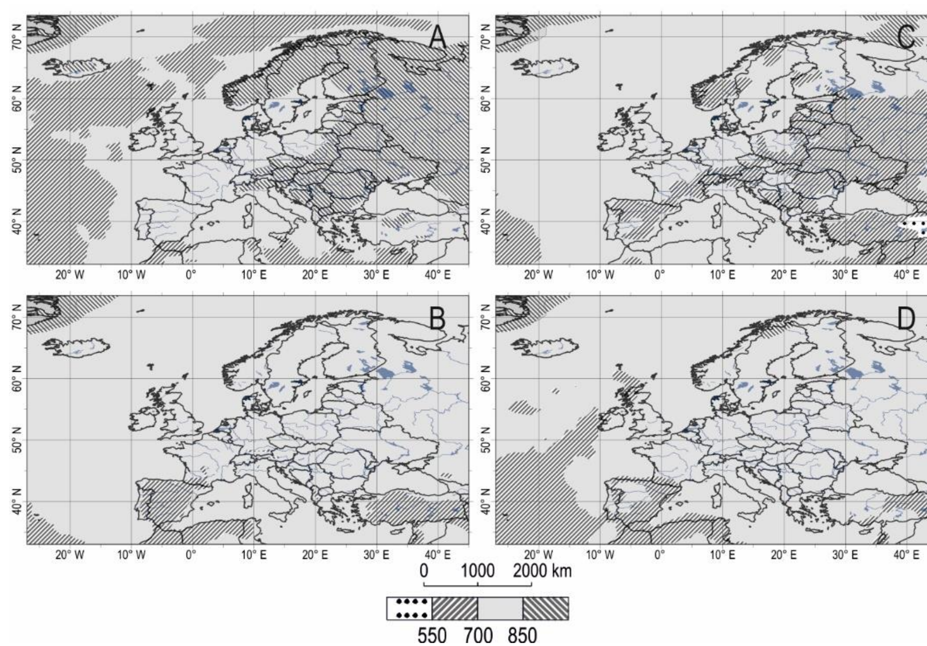

Mean height [hPa] of humidity inversion base
in selected months: A) JAN, B) APR, C) JUL, D) OCT

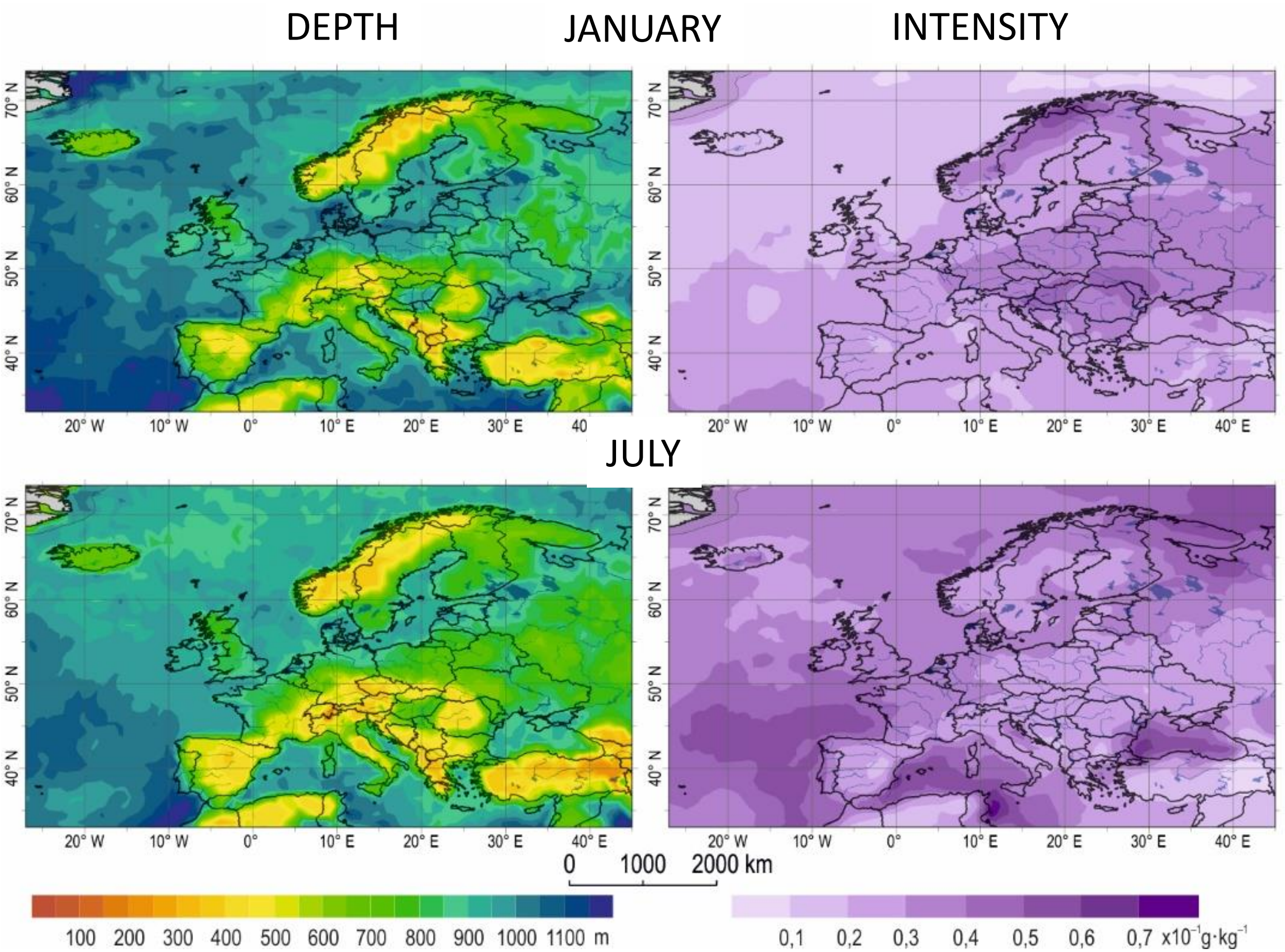

Mean humidity inversion depth and intensity

Moisture content regionalisation

TCWV, $TCWV_{\sigma}$, q_{950}, q_{850}, q_{700}, q_{500}, q_{σ}, RH_{950}, RH_{850}, RH_{700}, RH_{500}, RH_{σ} , $TCWV_{A}$

delimitation

- Global Moran's I statistics

$$I = \frac{n}{S_0} \cdot \frac{\sum_{i=1}^{n} \sum_{j=1}^{n} w_{i,j} (x_i - \bar{x})(x_j - \bar{x})}{\sum_{i=1}^{n} (x_i - \bar{x})^2}$$

$$S_0 = \sum_{i=1}^{n} \sum_{j=1}^{n} wi, j$$

x_i, x_j – values of compared features
$\bar{x}$ – mean value
$w_{i,j}$ – spatial weight between i and j

- k-means method
  - ✓ PCA
  - ✓ V-fold cross-validation
  - ✓ Pseudo-F statistics

validation

RMS Difference Ratio, RDR

$$RDR = \frac{\sum_{l=1}^{K} \sum_{k=1}^{K} N_k N_l}{\sum_{k=1}^{K} N_k (N_k - 1)} \cdot \frac{\sum_{k=1}^{K} \sum_{j=1}^{N_k} \sum_{i=1}^{N_k} S(x_{ik}, x_{jk})}{\sum_{l=1}^{K} \sum_{k=1}^{K} \sum_{j=1}^{N_l} \sum_{i=1}^{N_k} S(x_{ik}, x_{jl})}, \; l \neq k$$

Range Ratio, RR

$$RR = \frac{\max(x_i) - \min(x_i)}{\max(X) - \min(X)}$$

Moisture conditions

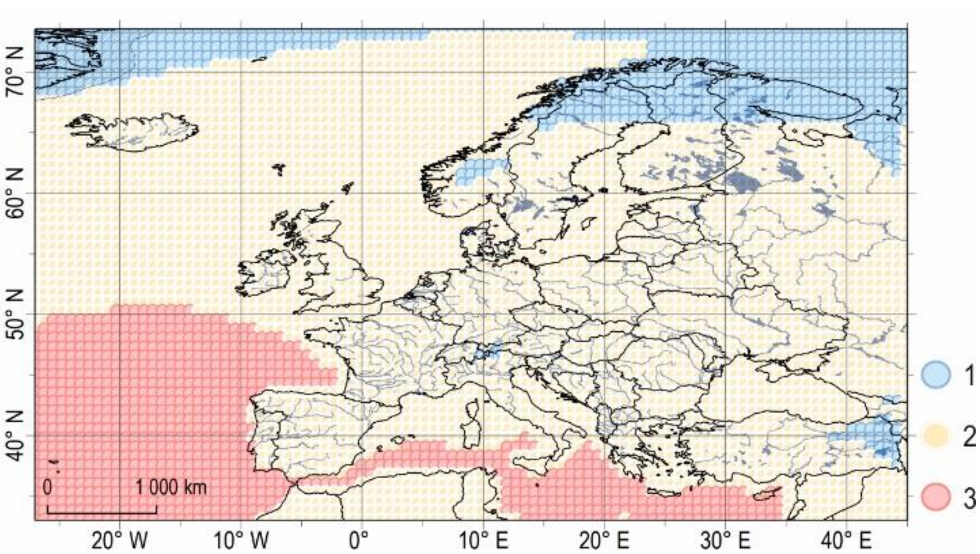

1 spatially homogenous low moisture content
2 no spatial homogeneity
3 spatially homogenous high moisture content

Moisture regions

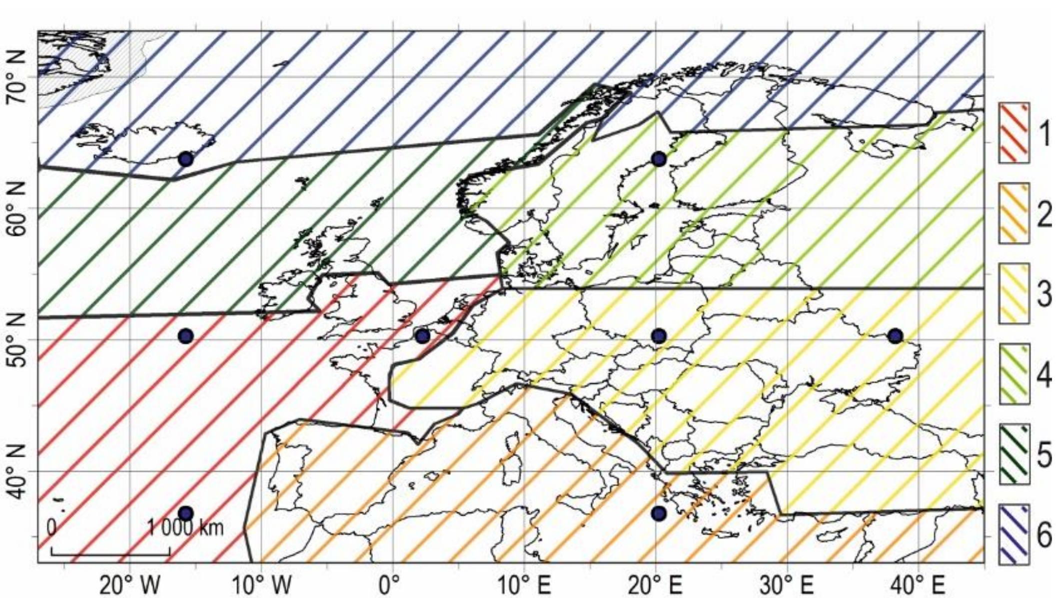

1 South Atlantic
2 Mediterranean
3 Mid–Continental South
4 Mid–Continental North
5 Mid–Atlantic
6 Arctic

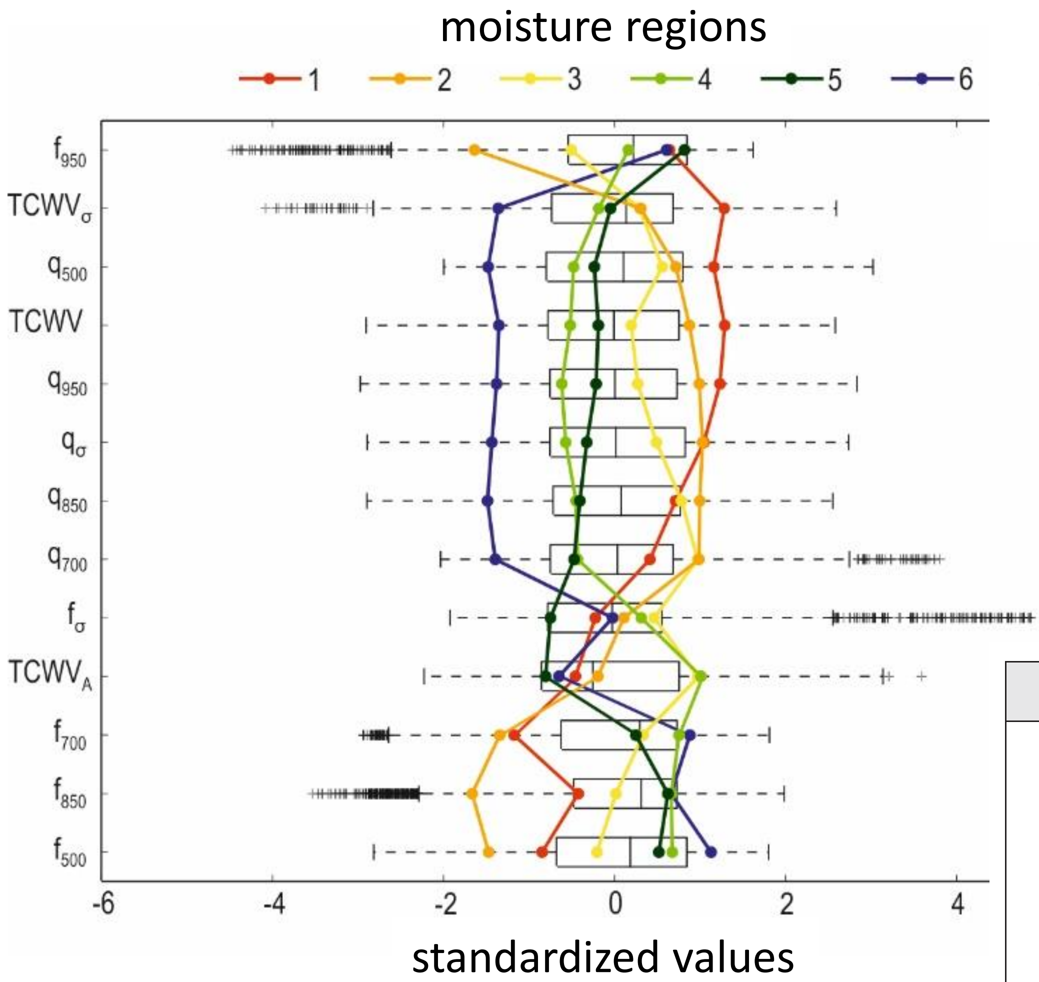

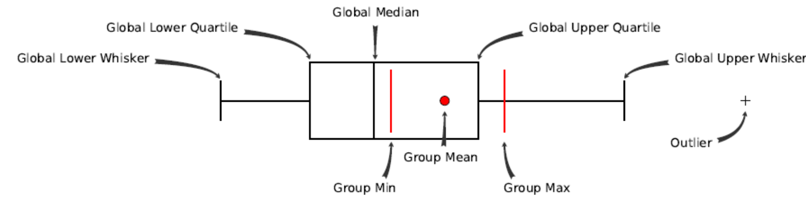

South Atlantic region

	variable		statistics $\bar{x}$	σ	min	max
1	q_{950}	$(g \cdot kg^{-1})$	7,0	0,959	5,3	9,3
2	q_{850}	$(g \cdot kg^{-1})$	4,4	0,404	3,6	5,5
3	q_{700}	$(g \cdot kg^{-1})$	2,2	0,134	1,9	2,6
4	q_{500}	$(g \cdot kg^{-1})$	0,8	0,062	0,7	0,9
5	q_{σ}	$(g \cdot kg^{-1})$	2,2	0,294	1,7	3,0
6	f_{950}	(%)	83,7	4,276	67,2	88,2
7	f_{850}	(%)	62,9	5,413	41,0	72,7
8	f_{700}	(%)	43,0	6,136	28,0	53,6
9	f_{500}	(%)	44,0	6,504	29,2	54,5
10	f_{σ}	(%)	15,6	1,232	13,2	19,3
11	TCWV	$(kg \cdot m^{-2})$	19,3	2,154	14,4	24,2
12	$TCWV_{\sigma}$	$(kg \cdot m^{-2})$	5,2	0,386	4,3	6,1
13	$TCWV_{A}$	$(kg \cdot m^{-2})$	11,6	0,978	9,5	15,7

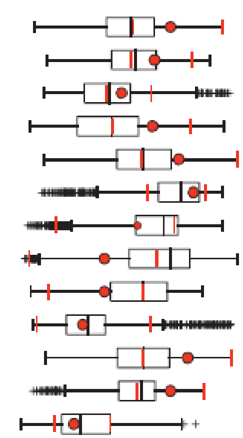

- SUMMARY 1 -

Analysis of temporal and spatial differences in water vapor content in the troposphere over Europe and the Northeastern Atlantic has shown large seasonal differences in the distribution of air water vapor over the course of the year. The largest **annual TCWV fluctuation** occurs **over land areas** and equals more than 20.0 kg·m^{-2} in the eastern part of the study area. Ocean areas are characterized by values more than 50% lower, while the eastern part of the Mediterranean Sea has a TCWV range of about 5.0 kg·m^{-2}.

The seasonality index expressed via the TCWV ratio for spring and autumn confirms **greater water vapor content in autumn**, although lower values are noted for water areas, where the air water vapor content is (on average) 20% lower in spring relative to autumn. This finding confirms the **significance of evaporation surfaces**.

Research results generated by the study confirm the existence of differences in the **vertical structure** of air water content in the troposphere over Europe and the Northeastern Atlantic. In this study, **six different vertical profile types were identified for land areas and four types for water areas**. These sometimes **differ substantially in terms of standard deviation**, which is linked with **variances in the physical characteristics of incoming air masses**. Research has also shown the presence of **moisture inversions** not only in areas north of 60°N but also in temperate and subtropical zones. Inversions can occur in two different forms – upper and lower.

Analysis of the spatial structures of water vapor content in the troposphere over Europe and adjacent to the west Atlantic Ocean has shown a strong regional pattern of moisture conditions in Europe and **the usefulness of TCWV as an indicator of the continental nature of the climate**. Six distinct moisture regions were identified in the study area. Their characteristics were defined independently in absolute terms and in terms of averages for the whole study area.

The role of atmospheric circulation

1) Relationships between moisture content and selected circulation variables:

TCWV – layer thickeness between 1000 hPa and 800 hPa (H_{1000}^{800}),

SHUM – geopotential height, eastward (u) and northward (v) wind component at pressure levels: 950 hPa, 850 hPa, 700 hPa, 500 hPa

2) PCA – EOF → dominant pressure patterns

Atmospheric circulation vs. moisture – Pearson's correlation coefficient between TCWV ($TCWV_{90}$) and EOFs

3) Atmospheric circulation typology: advection + pressure system

geostrophic wind direction (°)	symbol	circulation type
338–22	N	Na/Nc
23–67	NE	NEa/NEc
68–112	E	Ea/Ec
113–157	SE	SEa/SEc
158–202	S	Sa/Sc
203–247	SW	SWa/SWc
248–292	W	Wa/Wc
293–337	NW	NWa/NWc
–	–	Ca/Cc

4) Moisture transport intensity

$$IWVF = \sqrt{\left(\frac{1}{g_0}\int_0^1 uq\frac{\partial p}{\partial \eta}\ d\eta\right)^2 + \left(\frac{1}{g_0}\int_0^1 vq\frac{\partial p}{\partial \eta}\ d\eta\right)^2}$$

IWVF – integrated water vapour flux ($kg \cdot m^{-1} \cdot s^{-1}$)
q – specific humidity ($kg \cdot kg^{-1}$)
g 0 – gravity acceleration ($m \cdot s^{-2}$)
u – wind U component ($m \cdot s^{-1}$)
v – wind V component ($m \cdot s^{-1}$)
p – pressure (Pa)
η – hybrid vertical levels

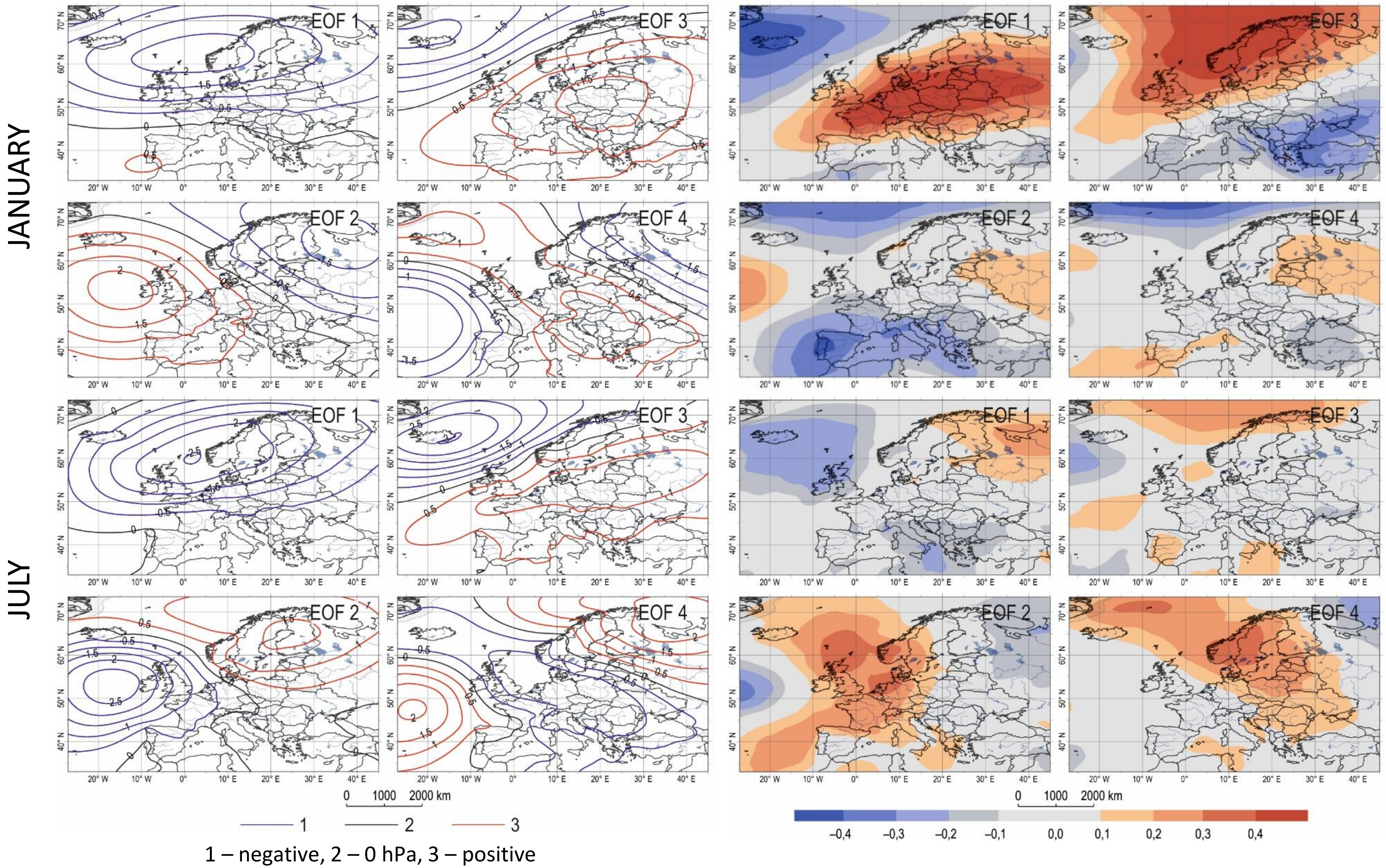

Spatial patterns of SLP anomalies (hPa, left) for leading EOF modes and their relationship with TCWV (Pearson's correlation coefficient, right) in selected months

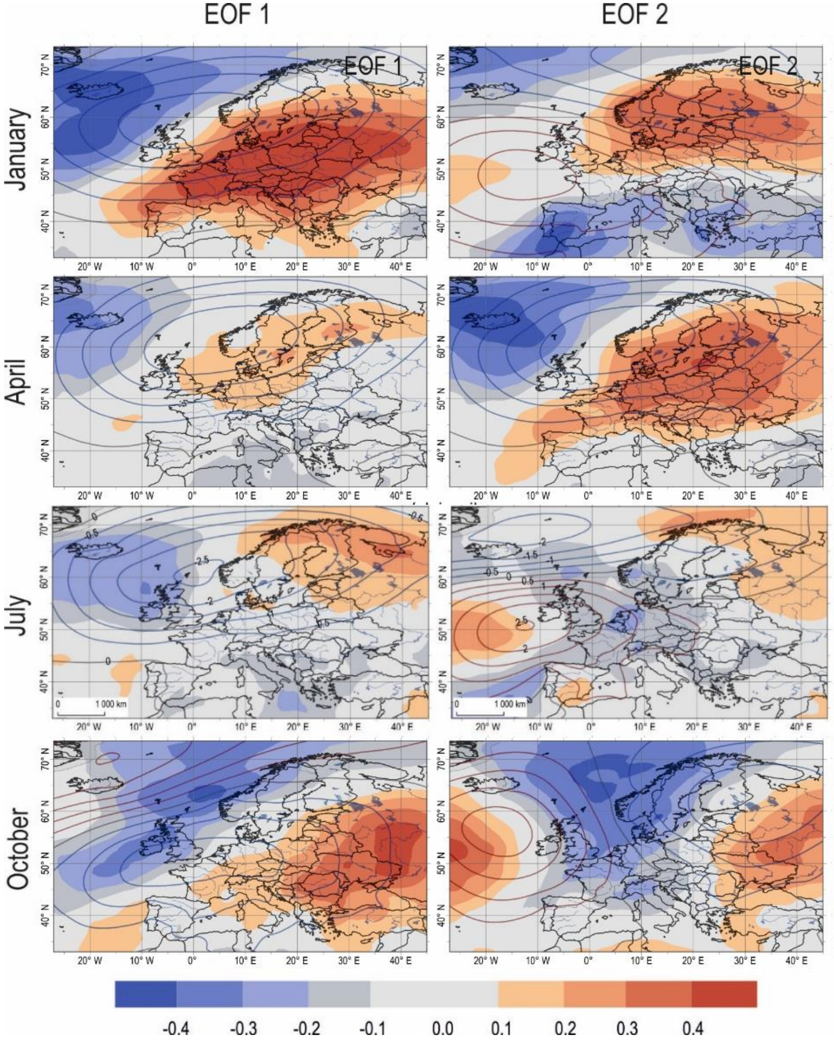

Spatial patterns of SLP anomalies (hPa, solid lines) for two leading EOF modes calculated for days with extremely high moisture content and their relationship with TCWV extremes (Pearson's correlation coefficient, in color) in selected months

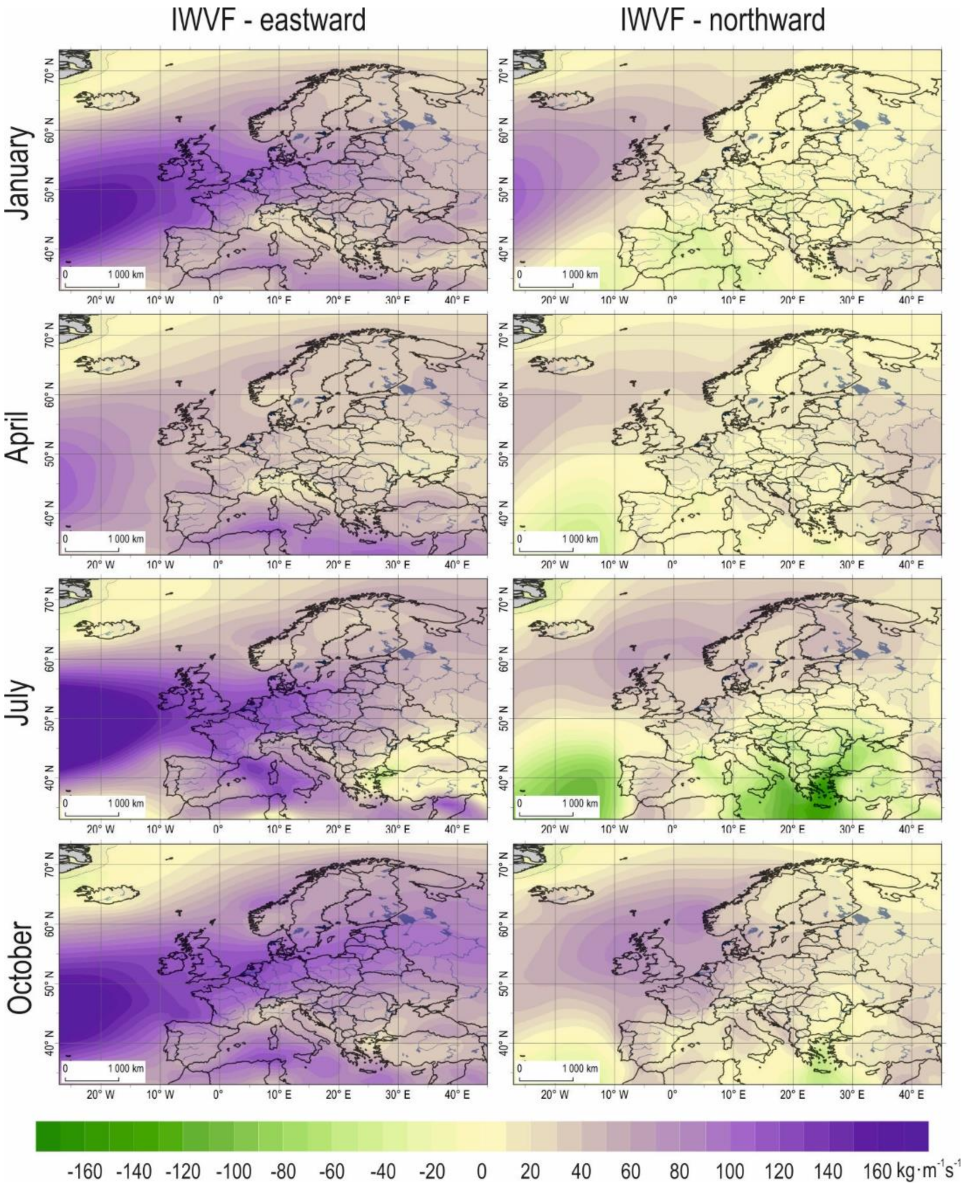

Vertically integrated water vapor flux, IWVF (kg·m^{-1}s^{-1}) for selected months

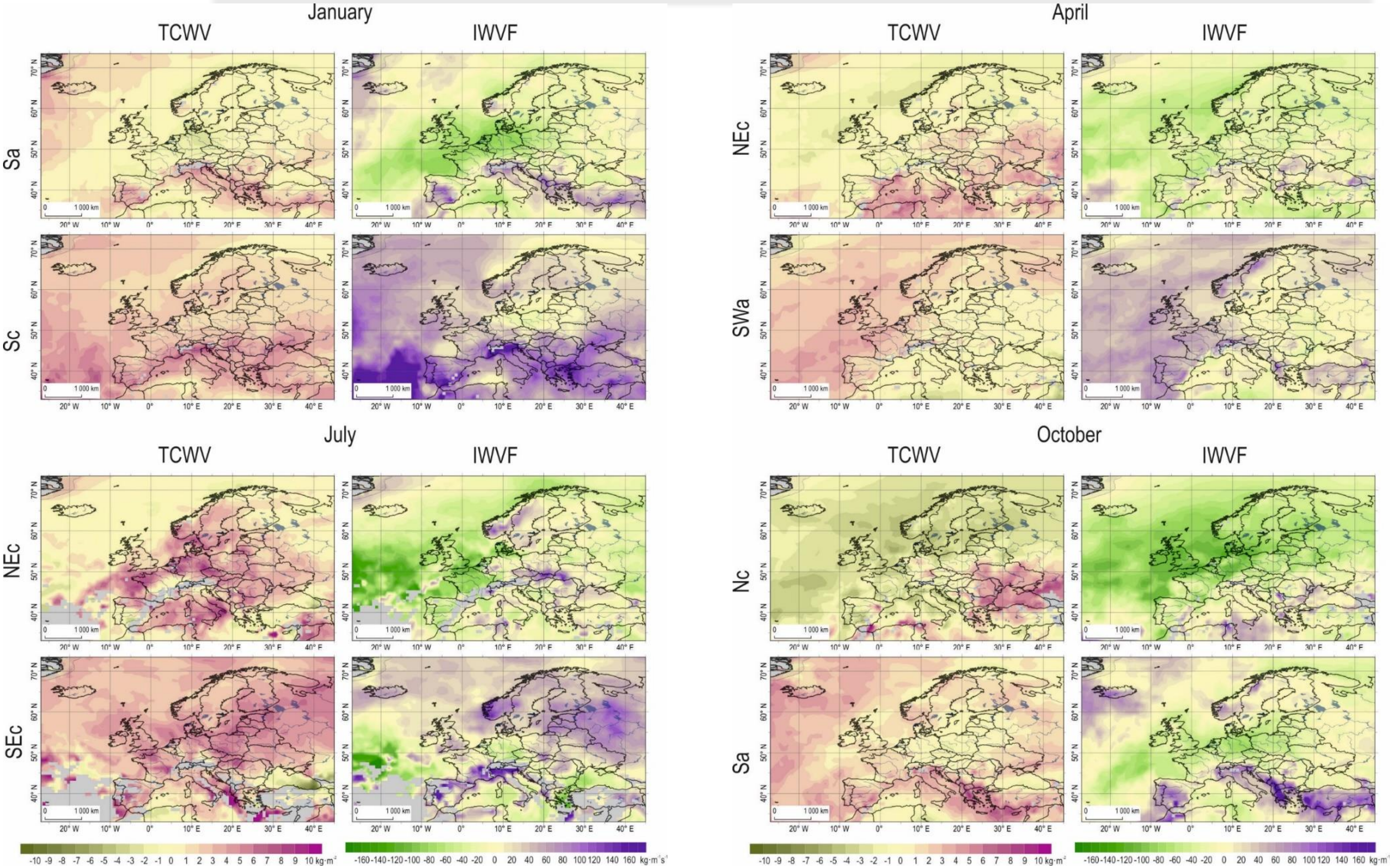

Anomalies of total column water vapor (TCWV) and total column water vapor flux (IWVF) for selected advection types in particular months – Grey shadows indicate absence of advection type occurrence

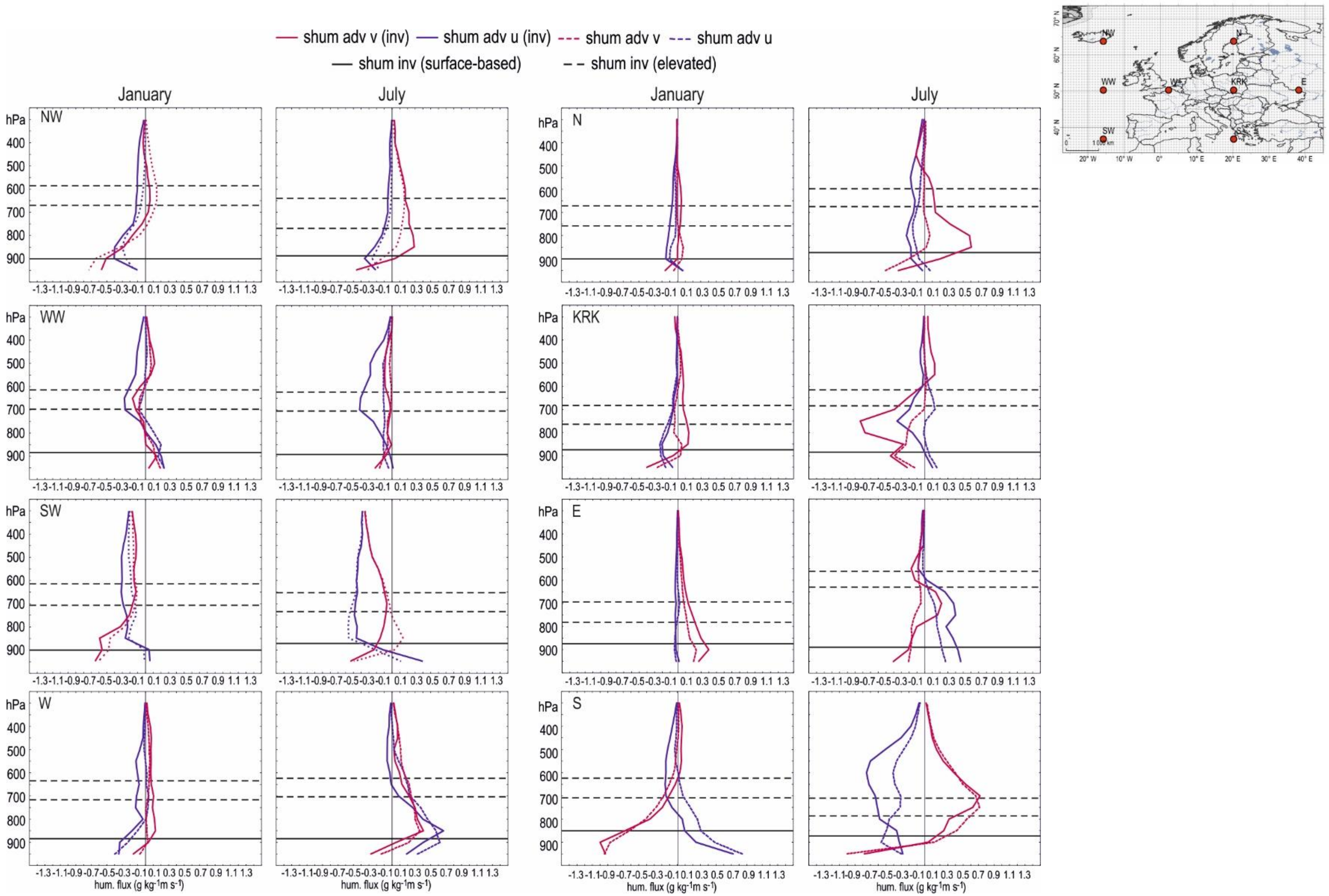

Climatologic mean profiles of specific humidity advective flux: eastward (u) and northward (v) during inversion (solid curve) and non-inversion (dashed curve) events at selected grid points

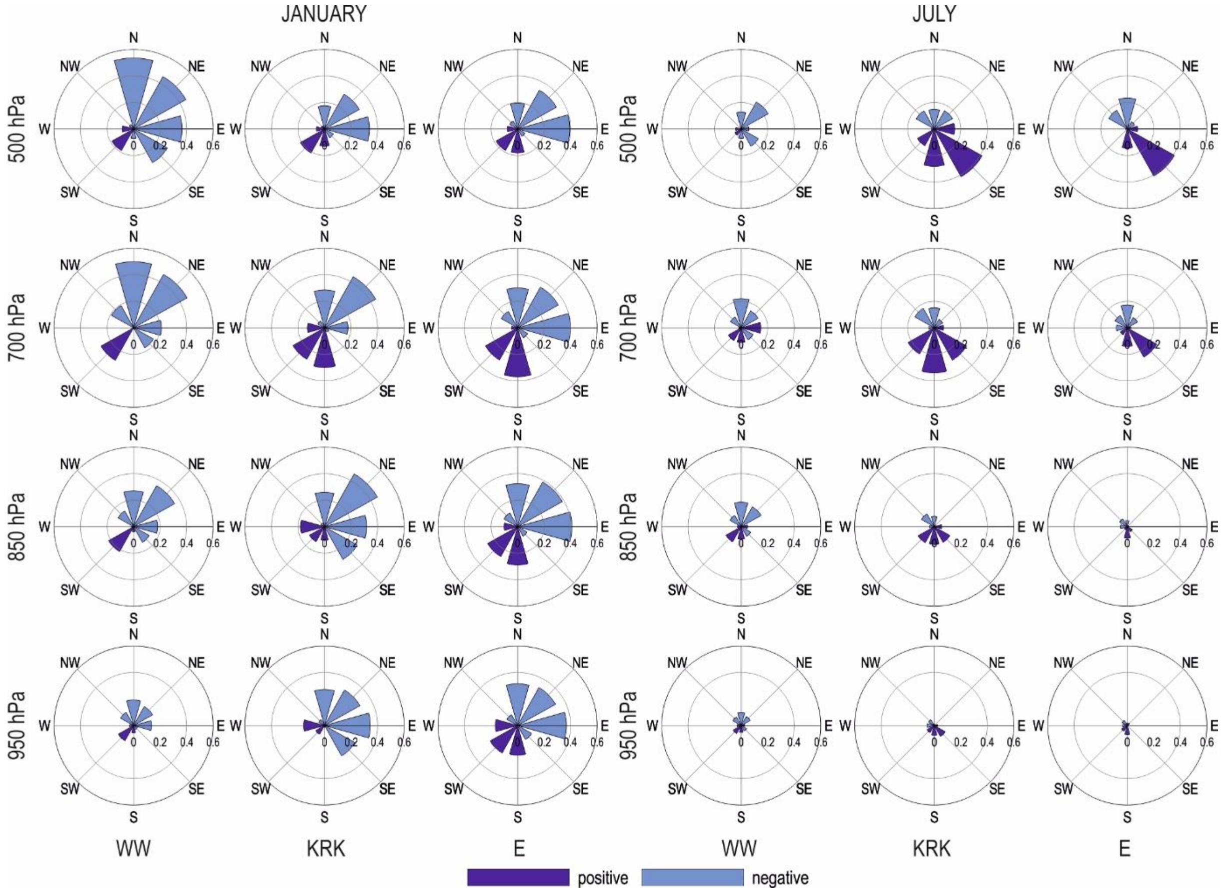

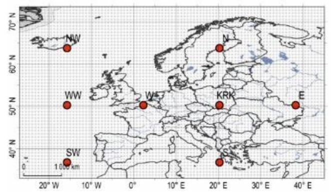

Specific humidity anomalies ($g \cdot kg^{-1}$) in advection directions (with respect to monthly mean, standardized) at selected pressure levels (1981-2015), selected grid points

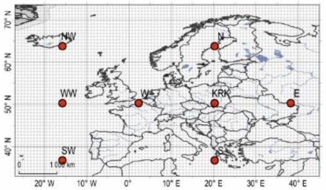

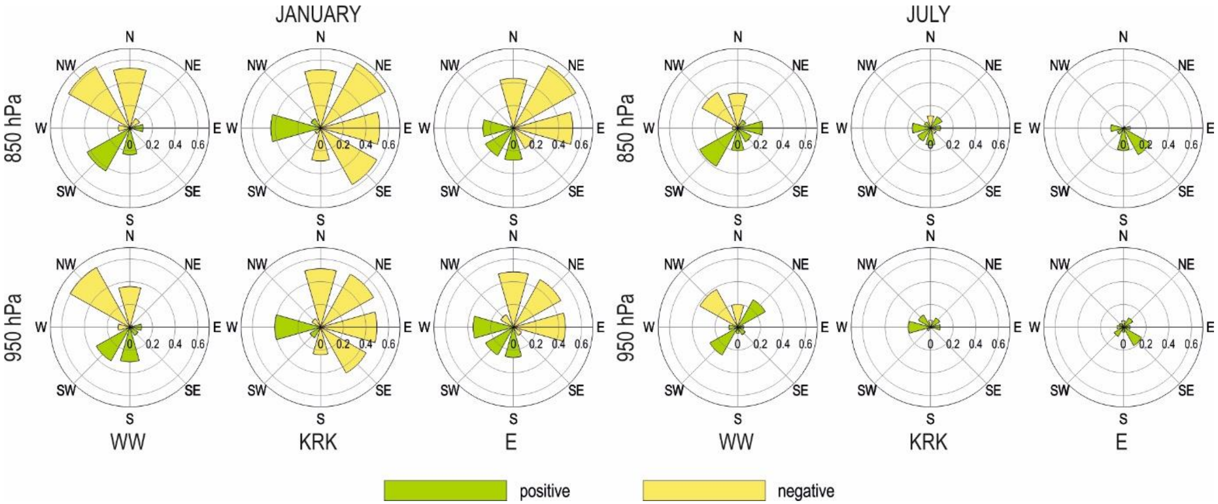

Specific humidity flux anomalies ($g \cdot kg^{-1} m \cdot s^{-1}$) in advection directions (with respect to monthly mean, standardized) at selected pressure levels (1981-2015), selected grid points

- SUMMARY 2 -

Analysis of the role of atmospheric circulation in the evolution of moisture conditions at the continental and local scales has shown that **atmospheric circulation** is often **important in the winter**, although water vapor content is affected by both pressure system type (key role of seasonal high) and the direction of advection – air rich in water vapor is transported from over the ocean in the direction of land thanks to **zonal circulation** (key role of drifting lows of extratropical areas) and in the northern direction.

The influence of atmospheric circulation impacts not only water vapor content in air but also its vertical structure, although the atmospheric boundary layer is most pronounced over land areas in the winter with the occurrence of anomalies associated with atmospheric circulation type. However, most of the study area **does not experience a relationship between atmospheric circulation and water vapor content in air in summer** (July). Research has also shown **a large moisture deficit in air masses on days with extreme TCWV values**, which suggests that summer atmospheric precipitation over Europe is rooted first and foremost in convection processes, while water vapor streams play a secondary role.

- CONCLUSIONS -

The problem of the spatial and seasonal distribution of air moisture in Europe is less often discussed in the research literature compared with e.g. air temperature and atmospheric precipitation. However, it is highly relevant from an environmental and hydrologic point of view. Air moisture is also an important element of meteorological and climatic models. The study area consisted of Europe – the smallest of all continents. Yet, Europe features highly complex air moisture conditions due to its geographic location, relief, and influence of large water bodies in the area. This applies to the surface of the Earth as well as lower tropospheric levels. The study attempted to identify this differentiation and also explain its causes wherever possible.

Climatologic analysis performed for the whole study area using homogeneous methods seems to be a good starting point for further analysis employing data with better temporal resolution as well as data featuring additional variables including remote sensing information such as satellite products. The accurate characterization of moisture fields is needed in order to parametrize climate and meso-meteorologic models for the purpose of improving cloud cover and precipitation forecasts.

Further research:

✓ Variability and change of the amount of water vapour in the troposphere

✓ Atmospheric rivers in Central Europe – the extra source of moisture

REFERENCES:

Wypych A., 2018, *Para wodna w troposferze nad Europą*, Instytut Geografii i Gospodarki Przestrzennej UJ, s. 200 (in Polish with and English summary: *Tropospheric moisture content over Europe*)

Wypych A., Bochenek B., Różycki M., 2018, *Atmospheric moisture content over Europe and the Northern Atlantic*, Atmosphere, 9(1), 18, doi:10.3390/atmos9010018.

Wypych A., Bochenek B., 2018, *Vertical Structure of Moisture Content over Europe*, Advances in Meteorology, ID: 3940503.